Journal of Hydrology 393 (2010) 265–273

Contents lists available at ScienceDirect

Journal of Hydrology

journal homepage: www.elsevier.com/locate/jhydrol

# On the value of hourly precipitation extremes in regional climate model simulations

Martin Hanel [a,b,*], T. Adri Buishand [a,1]

[a] Royal Netherlands Meteorological Institute (KNMI), PO Box 201, 3730 AE De Bilt, Netherlands
[b] Faculty of Environmental Sciences, Czech University of Life Sciences Prague, Kamýcká 129, Praha 6, Suchdol 165 21, Czech Republic

ARTICLE INFO

*Article history:*
Received 18 February 2010
Received in revised form 30 June 2010
Accepted 28 August 2010

This manuscript was handled by Konstantine P. Georgakakos, Editor-in-Chief, with the assistance of Rebecca Morss, Associate Editor

*Keywords:*
Hourly precipitation extremes
Regional climate model simulations
Nonstationary index-flood model
Radar rainfall

SUMMARY

Hourly precipitation extremes in the Netherlands in eight transient (1951–2099) and five ERA40 driven (1961–2000) regional climate model (RCM) simulations were analyzed. Generalized extreme value (GEV) distributions were fitted to the annual maximum amounts. Large differences were found between the estimated GEV parameters for the RCM simulations and those for an 11-year (1998–2008) high-quality radar data set. There were also large differences between the GEV parameters for different RCM simulations. The influence of the boundary conditions (ERA40 or a global climate model simulation for the present climate) on the extreme value distributions was in most cases small. A similar analysis for the daily precipitation extremes revealed much smaller differences between RCM simulations and a much better agreement with the results for the radar data. The increase in large quantiles of the daily maxima at the end of the 21st century in the transient RCM simulations was much smaller than that in the quantiles of the hourly maxima. For the latter, large differences were found between the changes from different RCM simulations, partly resulting from an increase in the GEV shape parameter in a number of RCM simulations. This increase in the shape parameter also largely explains the differences between the changes in large quantiles of the hourly and daily precipitation extremes.



## 1. Introduction

Changes in extreme precipitation due to climate change have received much interest during the last decade, mainly because of the direct impact on the hydrological regime and the frequency and severity of flooding. To assess possible future changes at the local scale, increased use has been made of the simulations of regional climate models (RCMs). Nowadays, there are already quite a few publications on daily precipitation extremes in RCM data (e.g., Buonomo et al., 2007; Durman et al., 2001; Fowler et al., 2007; Fowler and Ekström, 2009; Frei et al., 2006; Goubanova and Li, 2007). However, modeling of the rainfall–runoff dynamics in urbanized areas requires time-scales shorter than 1 day (e.g. Schilling, 1991; Berne et al., 2004). Lack of commonly available sub-daily RCM data has limited research on changes in short-duration precipitation extremes. The studies published so far consider only a very small number of RCM simulations. For instance, Grum et al. (2006) used changes in the 1-h precipitation statistics obtained from one RCM for a grid box in Denmark to alter observed point precipitation measurements in order to assess the climate change impact on a drainage network. Lenderink and van Meijgaard (2008) analyzed the changes in hourly precipitation maxima over Europe in one RCM simulation. Olsson et al. (2009) investigated 30-min precipitation at a grid box in Sweden in two RCM simulations. Onof and Arnbjerg-Nielsen (2009) used an hourly rainfall generator in combination with a random cascade disaggregator to downscale the information from an hourly RCM simulation to 5-min point precipitation.

Recently, the daily values of the hourly precipitation maxima over Europe from a relatively large number of RCM simulations conducted in the framework of the EU funded ENSEMBLES project (Hewitt and Griggs, 2004) have been archived. This enables the assessment of the ability of RCMs to simulate hourly precipitation maxima and the description of the uncertainty in future projections. In the present paper we compare the distributions of the 1-h and 1-day annual precipitation maxima in a number of RCM simulations conducted within the ENSEMBLES project with those from a unique high-quality radar data set in the Netherlands (Overeem et al., 2009b). Eight RCM simulations nested within transient global climate model (GCM) simulations and five RCM simulations driven by the ERA40 reanalysis (Uppala et al., 2005) are considered. For the GCM driven RCM simulations, the changes in the distributions of the annual precipitation maxima are also dealt with. The model developed by Hanel et al. (2009) for regional frequency analysis was used for statistical inference on precipitation maxima.

* Corresponding author at: Faculty of Environmental Sciences, Czech University of Life Sciences Prague, Kamýcká 129, Praha 6, Suchdol 165 21, Czech Republic. Tel.: +420 224382132.
*E-mail addresses:* hanel@fzp.czu.cz (M. Hanel), buishand@knmi.nl (T.A. Buishand).
[1] Tel.: +31 302206450.

0022-1694/$ - see front matter © 2010 Elsevier B.V. All rights reserved.
doi:10.1016/j.jhydrol.2010.08.024

The data and statistical model that have been used are introduced in Sections 2 and 3, respectively. In Section 4, the estimated GEV parameters from the RCM simulations for the present climate are compared with those from the radar data, and the changes in the GEV parameters and quantiles of the annual maximum distributions at the end of the 21st century are discussed. In Section 5, the main results are summarized and a number of concluding remarks are presented.

## 2. Data

Table 1 gives an overview of the 13 RCM simulations analyzed in this paper. These simulations were conducted with five RCMs. Eight of the RCM simulations were driven by transient runs of GCMs forced by the SRES A1B emission scenario and five by the 'perfect boundary' of the ERA40 reanalysis. The transient simulations were driven by ECHAM5 (Jungclaus et al., 2006), ARPEGE (Salas-Mélia et al., 2005), and three versions of HadCM3 (Collins et al., 2006) resulting from a perturbed physics ensemble experiment, i.e., HadCM3Q0 without parameter perturbations, HadCM3Q3, and HadCM3Q16 with parameter perturbations giving the lowest and highest global temperature response to external forcings, respectively. The precipitation extremes in the four ECHAM5 driven simulations are strongly correlated because of the common boundary conditions. Moreover, the differences between these simulations are caused by RCM biases. In contrast, the differences between the three transient RCA simulations are the result of differences between the boundary conditions.

All transient simulations we analyzed cover the period 1951–2099. The ERA40 driven simulations span the period 1961–2000. The data and information about the simulations are available in the archive of the ENSEMBLES project (http://ensemblesrt3.dmi.dk). The horizontal resolution is in all cases ≈25 km using the same rotated longitude–latitude grid. There are 65 grid boxes covering the Netherlands (Fig. 1).

The radar data set used as a reference for the present climate consists of 11 years (1998–2008) of 5 min data with a horizontal resolution of 2.4 km. These data were obtained from two C-band Doppler weather radars, one located in De Bilt in the middle of the country and one in Den Helder in the northwest of the country (see Fig. 1). After ground clutter removal, the data from both radars were combined into one composite, using a weighting factor depending on the distance to the radar. The raw radar precipitation amounts were adjusted using rain gauge data from an automatic network with 1-h precipitation amounts (≈1 station per 1000 km$^2$) and a manual network with daily precipitation amounts (≈1 station per 100 km$^2$). An extensive description of the adjustment procedure is given by Overeem et al. (2009b). These authors further showed that the average precipitation amounts and the frequency distribution of the 24-h precipitation amounts from the adjusted radar data were in good correspondence with those based on the manual rain gauge network. For the 1-h precipitation amounts from the adjusted radar data, however, an underestimation of the exceedance frequencies of extreme levels was found. This underestimation is caused by errors such as attenuation or changes in the vertical profile of reflectivity. The density of the automatic rain gauge network is too low to adjust for these errors. The systematic error of extreme hourly precipitation is considered further in Section 3.

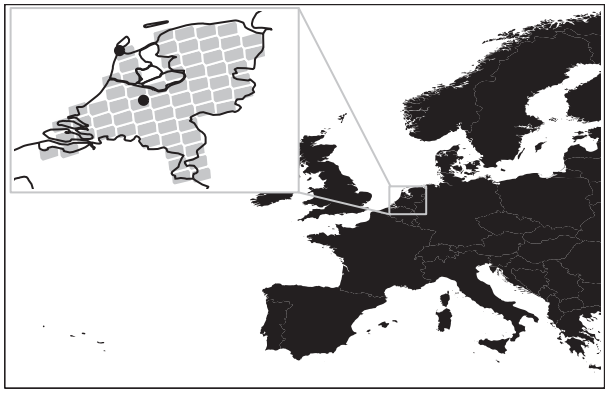

**Fig. 1.** The study area. The gray boxes in the inset figure represent the RCM grid boxes in the Netherlands, the black dots show the location of the two radars used for validation.

## 3. Methods

We assume that the 1-h and 1-day annual precipitation extremes follow a generalized extreme value (GEV) distribution. This distribution has often been used to model annual maximum precipitation from observed data and from RCM simulations (e.g., Fowler et al., 2007; Overeem et al., 2009a). The GEV distribution is defined by the distribution function:

$$F(x) = \exp\left\{-\left[1+\kappa\left(\frac{x-\xi}{\alpha}\right)\right]^{-\frac{1}{\kappa}}\right\}, \quad \kappa \neq 0,$$
$$F(x) = \exp\left\{-\exp\left[-\left(\frac{x-\xi}{\alpha}\right)\right]\right\}, \quad \kappa = 0, \tag{1}$$

with $\xi$, $\alpha$ and $\kappa$ the location, scale and shape parameter, respectively. The location parameter corresponds to the $1/e$ quantile of

**Table 1**
Overview of the RCM simulations.

| RCM | Acronym | Boundary | Source |
|---|---|---|---|
| RACMO2.1 (van Meijgaard et al., 2008) | RACMO_EH5<br>RACMO_E40 | ECHAM5<br>ERA40 | Royal Netherlands Meteorological Institute (KNMI) |
| REMO5.7 (Jacob et al., 2001) | REMO_EH5<br>REMO_E40 | ECHAM5<br>ERA40 | Max Planck Institute for Meteorology (MPI), Germany |
| HadRM3.0 (Jones et al., 2004) | HadRM_Q0<br>HadRM_E40 | HadCM3Q0<br>ERA40 | Met Office Hadley Centre, UK |
| HIRHAM5 (Christensen et al., 2007) | HIR_ARP<br>HIR_EH5<br>HIR_E40 | ARPEGE<br>ECHAM5<br>ERA40 | Danish Meteorological Institute (DMI) |
| RCA3.0 (Kjellström et al., 2005) | RCA_EH5<br>RCA_Q3<br>RCA_E40 | ECHAM5<br>HadCM3Q3<br>ERA40 | Swedish Meteorological and Hydrological Institute (SMHI) |
| | RCA_Q16 | HadCM3Q16 | Community Climate Change Consortium for Ireland (C4I) |

the distribution of the maxima. The return period associated to this quantile is $1/(1-1/e) \approx 1.58$ years. The location parameter strongly determines the mean, but does not influence the standard deviation and higher order central moments. The scale parameter is proportional to the standard deviation. The shape parameter controls the tails of the distribution with positive values implying a heavy upper tail. The case $\kappa = 0$ is known as the Gumbel distribution. For short-duration precipitation extremes the shape parameter is generally positive (e.g., Koutsoyiannis, 2004; Overeem et al., 2008). In the statistical model of Hanel et al. (2009), which is used here to assess the precipitation extremes in the RCM data, the scale parameter $\alpha$ is replaced by the dimensionless dispersion coefficient $\gamma = \alpha/\xi$. This dispersion coefficient is proportional to the coefficient of variation of the maxima.

Hanel et al. (2009) assume that in a predefined region (here the Netherlands) the precipitation maxima in a certain year are identically distributed at all grid boxes after scaling with a grid box-specific factor. This assumption, often used in regional frequency analysis, is usually referred to as the index flood assumption (Hosking and Wallis, 1997). For the GEV distribution it implies that both $\gamma$ and $\kappa$ are constant over the region of interest. Traditionally, the extremes have been scaled by their sample mean and median. However, for nonstationary data, it is convenient to consider the location parameter $\xi$. In the statistical model of Hanel et al. (2009) this parameter varies both over the grid boxes and over the years, whereas $\gamma$ and $\kappa$ only depend on time. The $T$-year quantile at grid box $s$ in year $t$ can then be represented as:

$$Q_T(s,t) = \xi(s,t) q_T(t), \tag{2}$$

where $\xi(s,t)$ is the location parameter at grid box $s$ in year $t$, and $q_T(t)$ is a common dimensionless quantile function:

$$\begin{aligned} q_T(t) &= 1 - \frac{\gamma(t)}{\kappa(t)}\left\{1 - \left[-\log\left(1-\frac{1}{T}\right)\right]^{-\kappa(t)}\right\}, \quad \kappa(t)\neq 0, \\ q_T(t) &= 1 - \gamma(t)\log\left[-\log\left(1-\frac{1}{T}\right)\right], \quad \kappa(t) = 0. \end{aligned} \tag{3}$$

Note that $q_T(t)$ is completely determined by the time-dependent dispersion coefficient $\gamma(t)$ and shape parameter $\kappa(t)$. A comprehensive derivation of the statistical model is given by Hanel et al. (2009).

Temporal variation in the GEV parameters is introduced by a time indicator $I(t)$. Simple relationships are used to link each GEV parameter to $I(t)$:

$$\xi(s,t) = \xi_0(s)\exp[\xi_1 I(t)], \tag{4}$$

$$\gamma(t) = \exp[\gamma_0 + \gamma_1 I(t)], \tag{5}$$

$$\kappa(t) = \kappa_0 + \kappa_1 I(t). \tag{6}$$

Note, that the trends in the GEV parameters $\xi(s,t)$, $\gamma(t)$ and $\kappa(t)$ are assumed to be constant over the region of interest. The exponential function in Eq. (4) ensures that the relative changes in the quantiles of the distribution are constant over the region as well. The exponential form of Eq. (5) restricts the dispersion coefficient to non-negative values. As a time indicator, the annual global temperature anomaly of the driving GCM is considered in the case of GCM driven simulations to represent the enhanced greenhouse gas forcing. Hanel et al. (2009) discussed the sensitivity of the changes in the GEV parameters and quantiles of the distribution to the time indicator $I(t)$ in Eqs. (4)–(6). These changes were almost the same for various choices of $I(t)$. For the ERA40 driven simulations, we assume stationarity of the precipitation maxima, i.e., $I(t) = 0$ for these simulations.

The parameters $\xi_0(s)$, $\xi_1$, $\gamma_0$, $\gamma_1$, $\kappa_0$ and $\kappa_1$ are estimated by a two-step maximum likelihood procedure (Hanel et al., 2009). The uncertainty of these estimates is assessed by a bootstrap procedure in which the precipitation maxima for a certain year (after removal of the temporal trend in the nonstationary case) are resampled simultaneously for all grid boxes to preserve the spatial dependence. To retain the dependence between RCMs driven by the same GCM simulation, bootstrap samples are based on the same sequences of years for all RCM simulations. Details on the uncertainty assessment are given in Appendix A.

As for the ERA40 driven simulations, stationarity of the precipitation maxima was also assumed for the radar data. The fact that these data were available for only 11 years hampers the estimation of the parameters in the index-flood model. In a simulation experiment, Overeem et al. (2009a) show that the full maximization of the likelihood for such short periods leads to seriously biased estimates of the dispersion coefficient and the shape parameter. These biases can be reduced by assuming that the location parameter is constant over a certain region, which also reduces the standard error of the estimated location parameter. Since systematic regional differences in the location parameter are small in the Netherlands, this parameter was taken to be constant over the whole country in a study of Overeem et al. (in press) on extreme-value modeling of areal precipitation. In that study, the GEV distribution was fitted to the annual maxima of area-average precipitation for area sizes $A$ of 6 km$^2$ (1 radar pixel) to 1700 km$^2$ (289 radar pixels) and for durations $D$ of 15 min to 24 h. The location parameter increases with increasing duration because the annual maximum for a given duration cannot be smaller than the annual maximum for a shorter duration. The dispersion coefficient decreases with increasing duration reflecting that the relative variability of the annual maxima is large at short durations. The dependence of the shape parameter on duration is not statistically significant. The annual maxima of area-average precipitation for a given duration tend to decrease if the area becomes larger. This leads to a reduction of all three GEV parameters with increasing area size. Overeem et al. (in press) used regression models to describe the dependence of each GEV parameter on $D$ and $A$. For the comparison with the RCM simulations in this paper, the values for $D = 60$ min and 24 h and $A = 625$ km$^2$ were taken from these models. The values of the location parameter were reduced by a factor of 1.15 to allow for the differences between running 1-h and 1-day maxima (radar data) and consecutive 1-h and 1-day maxima (RCM data). This kind of correction is well-known in the literature (Hershfield, 1961; NERC, 1975; van Montfort, 1990). A bootstrap procedure similar to that for the RCM data was used to determine the uncertainty of the GEV parameters from the radar data.

Overeem et al. (2009a) showed that the effective length of the radar dataset was 80 years for the 10-year quantile of the 24-h precipitation amounts at a radar pixel and 100 years for the 50-year quantile. This effective length increases for durations shorter than 24 h because of the weaker spatial association of precipitation for short durations. Overeem et al. (2009a) also compared the 10-year and 50-year quantiles from the radar dataset with those based on rain gauge data from 12 stations that were evenly distributed over the Netherlands and had at least 29 years of data. For $D = 24$ h, the quantiles from the radar data were somewhat larger (7–9%), mainly because the 1998–2008 period is a rather wet period. However, for $D = 1$ h the quantiles from the radar data turned out to be smaller (6–8%). This difference is partly due to the remaining errors in the radar dataset, which could not be adjusted with a relatively sparse network of hourly precipitation measurements. The GEV location parameter for the 1-h maxima from the radar dataset was 14% lower than the estimate from rain gauge data for the same 11-year period.

Overeem et al. (in press) compared the reduction of the quantiles of the annual maximum distributions with increasing area size with the areal reduction factors from dense rain gauge networks in the literature. For a return period of two years the areal reduction factors obtained from the regression models for the GEV parameters were comparable to those in the UK Flood Studies Report (NERC, 1975). Further, a larger areal reduction effect was obtained for longer return periods, which is consistent with the study of Bell (1976) for precipitation data in the UK.

## 4. Results

### 4.1. Precipitation extremes for the present climate

Fig. 2 gives boxplots of the estimates of the GEV parameters $\xi$, $\gamma$, and $\kappa$ as obtained from 1000 bootstrap samples for the 1-h (Fig. 2a–c) and 1-day (Fig. 2d–f) annual precipitation maxima for the present climate. For the GCM driven simulations, the estimated values were derived from Eqs. (4)–(6) using the average annual global temperature anomaly in the period 1961–1990 as $I(t)$. The results are not much different if the temperature anomaly is taken for the period 1961–2000 (reference for the ERA40 reanalysis) or 1998–2008 (reference for the radar data). The estimates of the location parameter were averaged over the 65 grid boxes in the Netherlands.

For the 1-h maxima, the majority of the RCM simulations underestimate the location parameter (Fig. 2a) by 30–40% with respect to the radar data. For the REMO simulations the underestimation is less than 10%. Nearly all box plots are outside the confidence intervals for the radar data. This points to statistically significant biases even though the radar data refer to a rather short period. Surprisingly, there are large differences among the RCA simulations. While RCA_EH5 and RCA_E40 overestimate the location parameter by about 30%, this parameter is more than twice as large as that from the radar data in the RCA_Q3 simulation, and RCA_Q16 underestimates the location parameter by 40%. In Section 3, it was noted that the location parameter of the 1-h precipitation maxima at a radar pixel was underestimated by 14%, which may also apply to the values from the radar data in Fig. 2a. This underestimation is, however, small compared to the differences between the estimated location parameter for most RCM simulations and that from the radar data. Nevertheless, the underestimation by the radar implies that the bias in the RCA_EH5 and RCA_E40 simulations is in fact much smaller than Fig. 2a suggests. A serious overestimation of the dispersion coefficient (30–60%) is found in the RACMO, REMO, and HadRM simulations, while this parameter is reasonably reproduced in the HIRHAM and RCA simulations (Fig. 2b). The same holds for the shape parameter (Fig. 2c): a serious overestimation (0.2–0.4) in the case of RACMO, REMO, and HadRM and reasonable values for HIRHAM and RCA. Note, that values of the shape parameter larger than 1/3 (as found for RACMO, REMO, and HadRM) imply a very heavy tailed distribution with infinite skewness. Apart from the two RCA simulations driven by the two perturbed versions of the HadCM3

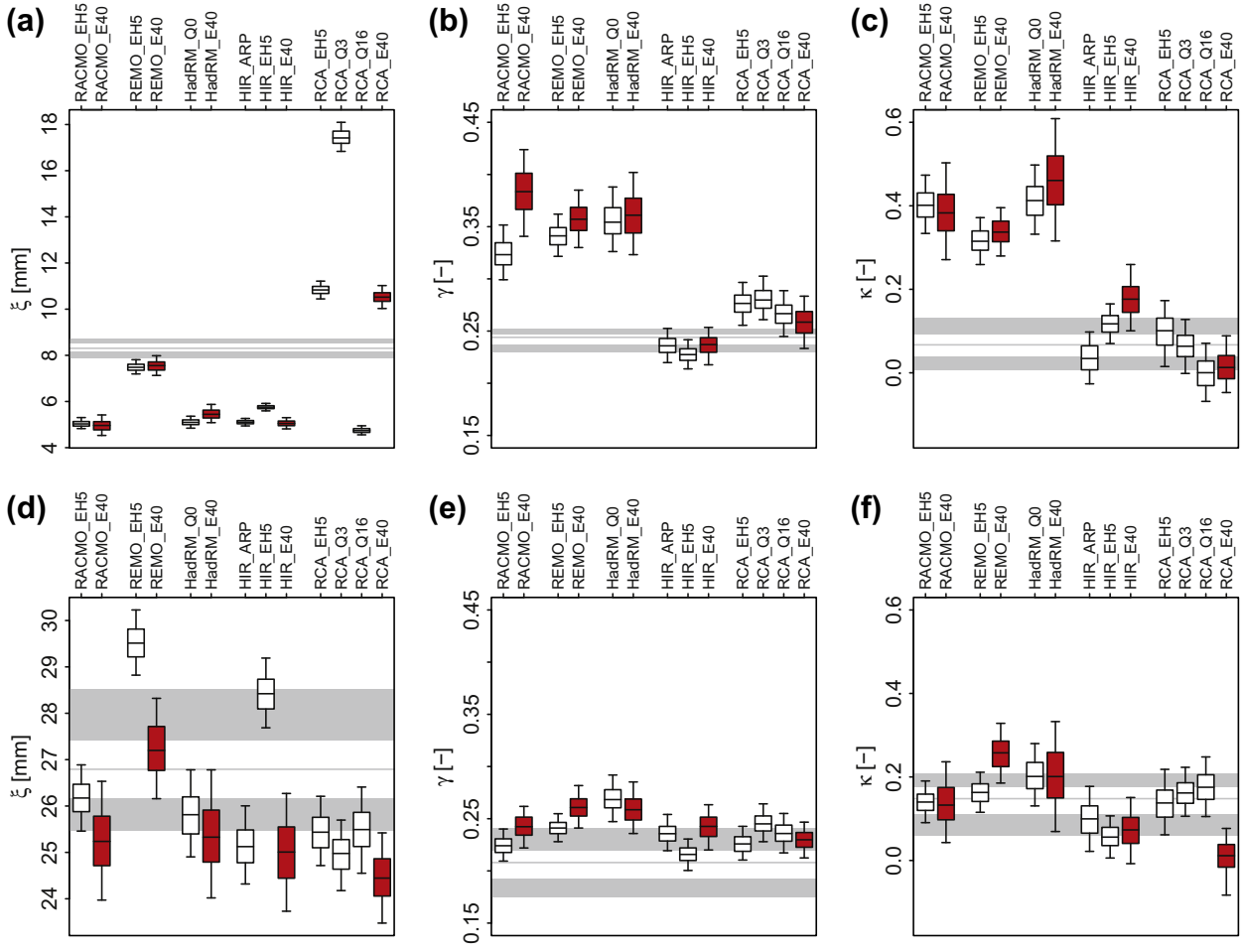


**Fig. 2.** Estimates of the GEV parameters for the (a–c) 1-h and (d–f) 1-day annual precipitation extremes for the present climate. The open boxes represent the values for the transient RCM simulations and the filled boxes the ERA40 driven simulations. The large gray box in the background shows the estimates from the radar data. The boxplots were obtained from 1000 bootstrap samples and the 5th, 25th, 50th, 75th, and 95th percentiles of these bootstrap samples are indicated.

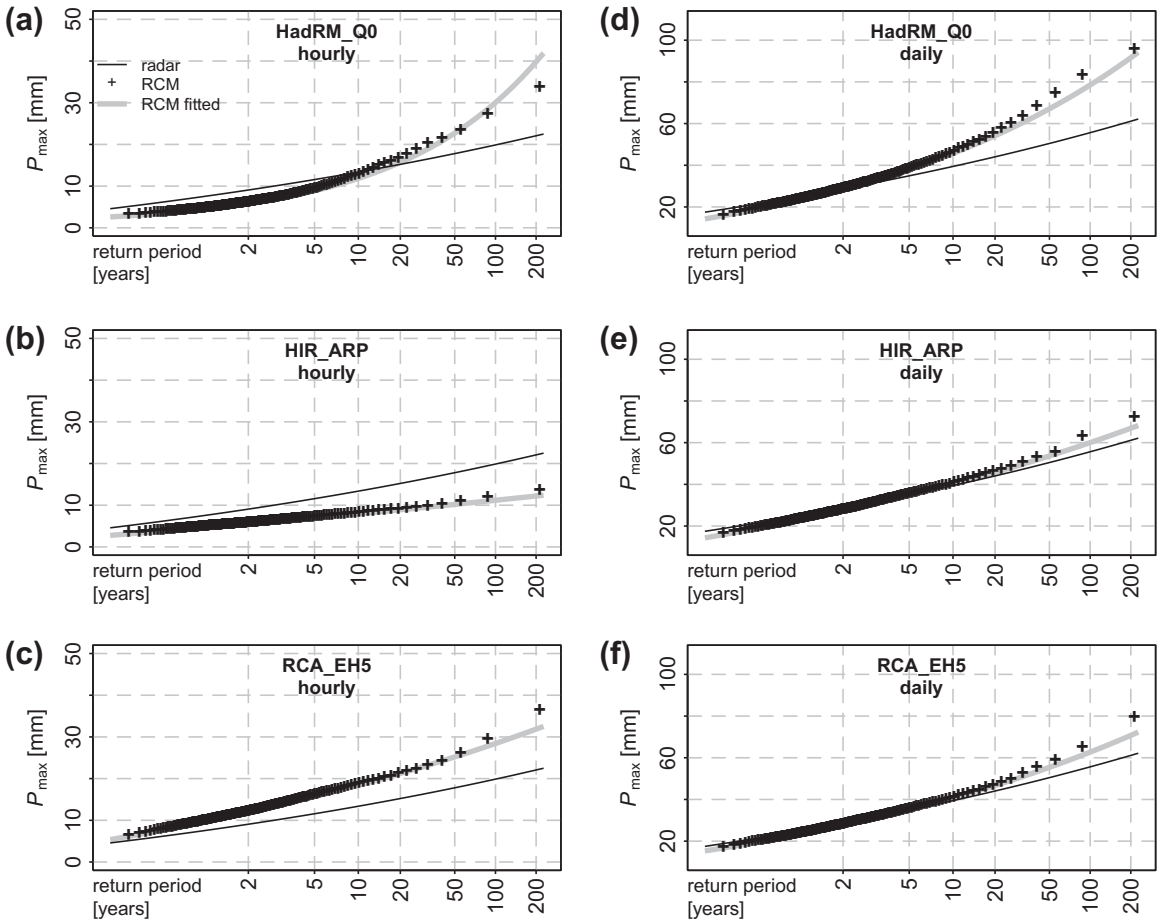


**Fig. 3.** Quantile plots of the (a–c) 1-h and (d–f) 1-day annual precipitation extremes ($P_{MAX}$) in the HadRM_Q0, HIR_ARP and RCA_EH5 simulations compared with the quantiles from the fitted GEV model and those from the radar data. The plots for the RCM simulations are average plots for the 65 grid boxes in the Netherlands.

model, there is little difference between the estimated GEV parameters for the ERA40 and GCM driven runs, indicating that the biases are largely due to the precipitation parameterization in the RCM rather than the driving boundary conditions (GCM, ERA40).

The GEV parameters for the 1-day precipitation maxima are in general much better reproduced in the RCM simulations. For all RCM simulations, the bias in the location parameter is less than 10% (Fig. 2d), and the bias in the shape parameter is lower than 0.2 (Fig. 2f). The dispersion coefficient is, however, overestimated by 10–40% (Fig. 2e).

These biases are comparable to those found by Hanel and Buishand (2010) for the summer maxima over the Dutch part of the Rhine basin (almost two-thirds of the Netherlands) in a larger number of transient RCM simulations from the ENSEMBLES project. The summer season is the season in which most heavy precipitation occurs (summer showers). For the radar data the 24-h maxima occurred mostly in the period July–December and the 60-min maxima mostly in the period June–September (Overeem et al., 2009a). The ERA40 and ECHAM5 driven simulations show the same behavior. Since the biases in the daily summer maxima and daily annual maxima are comparable in the ECHAM5 driven simulations for this region, similar results as for the annual maxima would have been obtained if the hourly and daily maxima in these RCM simulations were compared for the summer season only. The extremes in the other RCM simulations are more evenly distributed over the year. This holds both for the 1-day and 1-h maxima. Although the occurrence of extremes in the HadRM_Q0 simulation is less concentrated in the summer season than in the HadRM_E40 simulation, the biases in the GEV parameters for these simulations are comparable. This also applies to the HIR_ARP, HIR_EH5 and HIR_E40 simulations.

For the radar data, the confidence intervals for $\xi$ and $\gamma$ in Fig. 2 are relatively wide for the 1-day annual precipitation extremes. This is partly due to the larger spatial association of 1-day precipitation. For the uncertainty of the location parameter, the increase in the GEV scale parameter with increasing duration is also important. The confidence intervals for the shape parameter are the same for the 1-h and 1-day precipitation maxima from the radar data because the duration was not included in the regression model for this parameter (see Overeem et al., in press). For the 1-h precipitation extremes from the radar data, the widths of the confidence intervals for $\gamma$ and $\kappa$ strongly depend on the value of the shape parameter (a large value of $\kappa$ implies large uncertainty). The confidence intervals represent the uncertainty due to the availability of a limited amount of data. Multi-decadal variability is not taken into account. Further, exceptional years may have a considerable impact on the width of the confidence interval. For the 24-h maxima at a radar pixel, Overeem et al. (2009a) showed that the estimated uncertainty was reduced by about 20% if the year 1998 was omitted.

### 4.2. Goodness of fit

The Anderson–Darling test for (nonstationary) spatially correlated data on a grid (Hanel et al., 2009) did not reveal any lack of fit of the statistical model. The adequate fit of the GEV distribution

is also clear from Fig. 3 which compares quantile plots of the 1-h (Fig. 3a–c) and 1-day (Fig. 3d–f) precipitation extremes in the HadRM_Q0, HIR_ARP, and RCA_EH5 simulations with the quantiles from the fitted GEV model and the radar data. To produce these quantile plots, the trends with respect to the period 1961–1990 were first removed from the annual maxima, and then the quantiles of the adjusted annual maxima ($P_{MAX}$) were averaged over the 65 grid boxes in the Netherlands. The trend removal and area averaging are fully described in Appendix A. For the HadRM_Q0 and RCA_EH5 simulations, the largest 1-h precipitation amounts are plotted far above the line representing the quantiles from the radar data. These maxima are not much different in the two RCM simulations. The differences in the shape of the distribution are mainly determined by the less extreme events. For the HIR_ARP simulation, all quantiles of the 1-h precipitation maxima are smaller than those from the radar data set. The representation of the 1-day precipitation maxima is much more adequate. Only the quantiles from the HadRM_Q0 simulation considerably exceed those from the radar data for return periods longer than 10 years.

### 4.3. Projected changes in precipitation extremes

The estimated changes in the GEV parameters between the periods 1961–1990 and 2070–2099 for the transient RCM simulations are given in Fig. 4 together with the ensemble mean changes. For the 1-h maxima all three GEV parameters increase (Fig. 4a–c). The relative increase in the location parameter and the dispersion coefficient is on average 18% and 14%, respectively, the average absolute increase in the shape parameter is 0.11. There are, however, large differences among RCMs ranging from almost no change to an increase about twice as large as the ensemble mean change. In particular, the HIR_ARP and HIR_EH5 simulations exhibit a relatively large increase in both the dispersion coefficient and the shape parameter, which is caused by the occurrence of a number of exceptional precipitation maxima in the second half of these simulations. Very large events are also found in the second half of the RCA_Q16 simulation which has the largest increase in the shape parameter. For the 1-day maxima (Fig. 4d–f), there is on average a 14% increase in the location parameter and a 7% increase in the dispersion coefficient, while the shape parameter decreases slightly (−0.01).

Fig. 5a shows the ensemble mean relative changes in the quantiles of the distribution of the 1-h maxima between the periods 1961–1990 and 2070–2099. The changes in the lower quantiles are determined by the changes in the location parameter, thus up to the 2-year quantile there is an increase of about 15%. However, as the return period gets longer, the increase in the location parameter is enforced by the increase in the dispersion coefficient and the shape parameter leading to very large increases (45–60%) at return periods longer than 50 years. The uncertainty in this ensemble mean change is, however, considerable. In addition, there are large differences between the relative changes in large quantiles in the eight transient RCM simulations. The smallest increase (10%) is projected by HadRM_Q0, and the largest (110%) by HIR_EH5. The differences can partly be attributed to the increase in the shape parameter found in a number of RCM

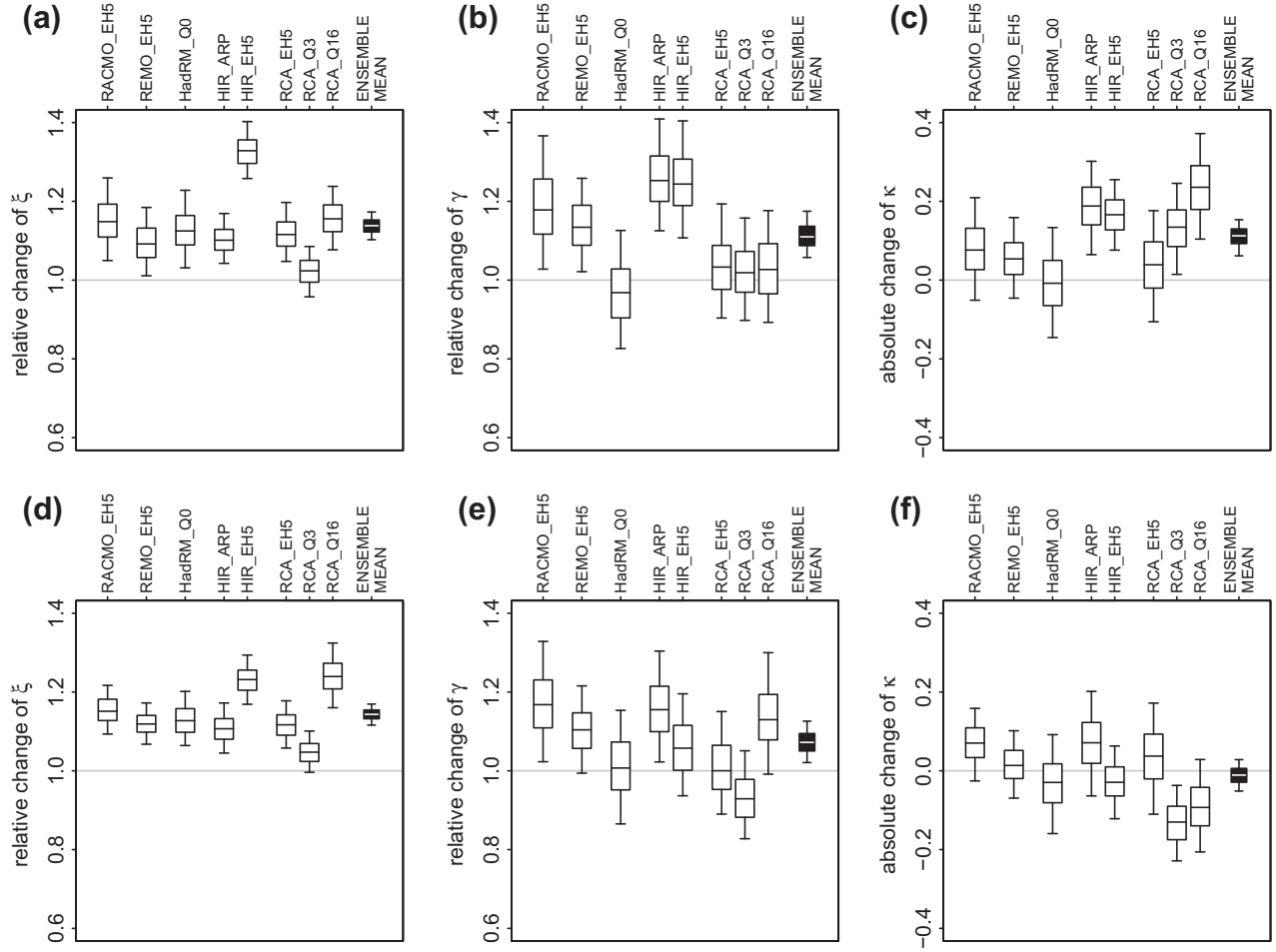


**Fig. 4.** Changes in the GEV parameters for the (a–c) 1-h and (d–f) 1-day annual precipitation extremes between the periods 1961–1990 and 2070–2099. The boxplots were obtained from 1000 bootstrap samples and the 5th, 25th, 50th, 75th, and 95th percentiles of these bootstrap samples are indicated.

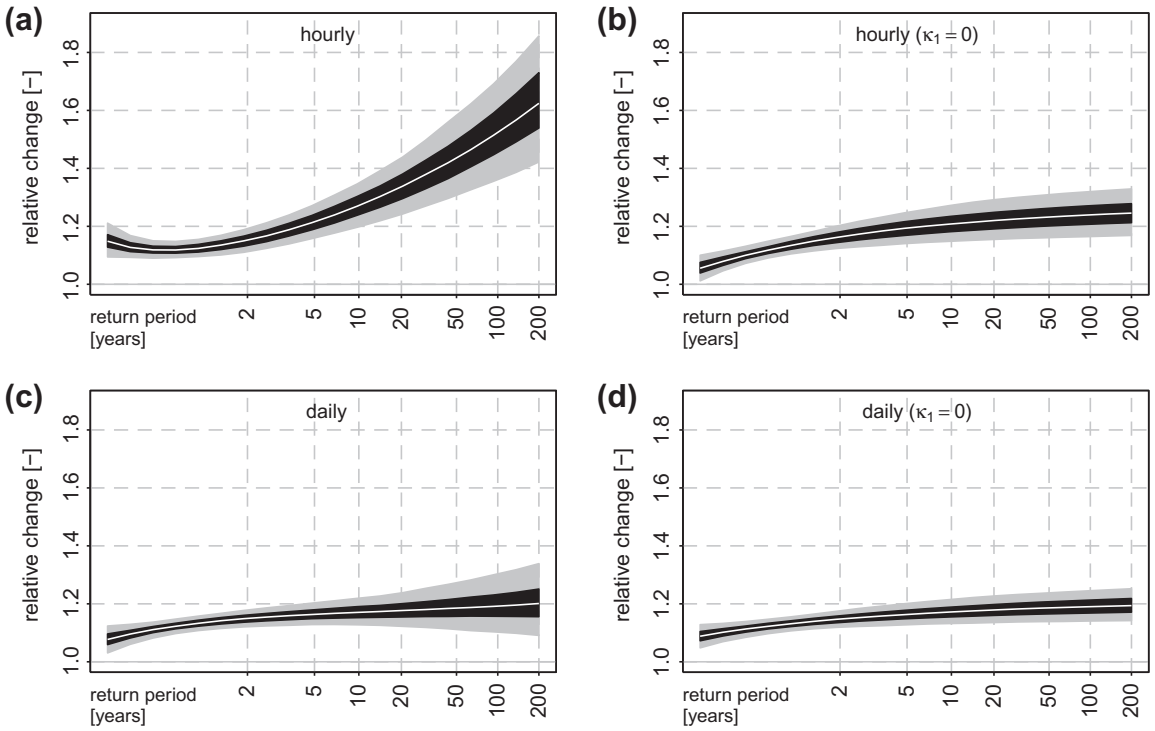


**Fig. 5.** Ensemble mean relative changes in the quantiles of the annual maximum distribution between the periods 1961–1990 and 2070–2099 for the 1-h and 1-day precipitation amounts for (a and b) the 1-h precipitation amounts, assuming a time-varying shape parameter (a) and a constant shape parameter (b), respectively, and (c and d) the same for the 1-day precipitation amounts. The uncertainty bands were obtained from 1000 bootstrap samples and the 5th, 25th, 50th, 75th, and 95th percentiles of these bootstrap samples are indicated.

simulations (Fig. 4c). To explore the impact of this increase on the changes in the quantiles, we refitted the statistical model assuming that the shape parameter is constant in time, i.e. with $\kappa_1 = 0$ in Eq. (6). Fig. 5b shows that this leads to a strong reduction of the increase in large quantiles and the uncertainty of this increase. The uncertainty band is outside the uncertainty band in Fig. 5a at long return periods due to the significant increase in the shape parameter in a number of RCM simulations.

Considering the average temperature increase over the Netherlands between the periods 1961–1990 and 2070–2099 from the RCM simulations (2.8 °C), the increase in 1-h extreme precipitation for long return periods becomes ≈18% per degree of warming. This is far beyond the value expected from the Clausius–Clapeyron relation (≈7%) and also above the value (14%) that was reported by Lenderink and van Meijgaard (2008) for the RACMO_EH5 simulation in large parts of Europe and observations in De Bilt in the Netherlands. The increase is, however, reduced to ≈9% per degree of warming if the shape parameter is kept constant.

The quantiles of the distribution of the 1-day maxima (Fig. 5c) increase with increasing return period for return periods shorter than 20 years owing to the increase in the location parameter and the dispersion coefficient. For larger quantiles, there is a more or less constant increase of about 19%. This corresponds to a 6.8% increase per degree of warming, which is close the value expected from the Clausius–Clapeyron relation. The average changes are similar if no change in the shape parameter is assumed (Fig. 5d), although the uncertainty of the changes in large quantiles is considerably reduced in that case.

## 5. Conclusions

The present study revealed that the distribution of the RCM simulated 1-h precipitation extremes in many cases strongly deviates from that of the radar data. The negative bias in the location parameter which is inherent in the majority of the considered RCM simulations implies that the simulated maxima tend to be too low. However, for the RACMO, REMO, and HadRM simulations the effect of the underestimation of the location parameter is outbalanced by a serious overestimation of the dispersion coefficient and shape parameter leading to a positive bias at long return periods. The positive bias in the location parameter in the case of the RCA_EH5 and RCA_Q3 simulations leads to an overestimation of all quantiles. In general, the skill of each simulation in modeling 1-h precipitation maxima is largely determined by the RCM. However, the value of the location parameter can be affected by the boundary conditions as well (see the RCA simulations in Fig. 2a). In contrast to the 1-h precipitation extremes, the distribution of the 1-day precipitation extremes is simulated quite well by the RCMs. This suggests that the underestimation of the location parameter for the hourly precipitation extremes is compensated by a stronger persistence of moderately large hourly values in the RCM simulations. Persistence at more extreme levels can, however, be limited by available moisture. This restricts the amount of precipitation on the daily time scale. The better reproduction of the distribution of the 1-day precipitation extremes applies to RCM simulations that preserve the observed seasonal cycles of the 1-h and 1-day precipitation extremes as well as to the RCM simulations that do not preserve this seasonal cycle.

The relative change in the quantiles of the 1-h precipitation extremes is influenced by the increase in all GEV parameters leading to very large increases in large quantiles, i.e., a 45–60% increase at return periods from 50 to 200 years. The quantiles of the 1-day precipitation extremes increase as well, however, this increase is only ≈20% for long return periods. The different behavior of the changes in large quantiles between the 1-h and 1-day precipitation extremes is caused by a significant increase in the shape parameter of the 1-h maxima in several RCM simulations, which is not found for the 1-day maxima.

Although the projections of hourly precipitation extremes are often needed for climate change impact assessment, the large deviations of the distribution of the simulated 1-h maxima from that obtained from the radar data questions the ability of a number of RCMs to represent (convective) precipitation properly at the hourly scale. Direct use of the projections from these models should therefore always be made with care. Alternative methods should be considered as well. Given the very large uncertainty in the projected changes in hourly precipitation extremes between different RCM simulations, multi-model assessment is necessary.

## Acknowledgements

We acknowledge the ENSEMBLES project, funded by the European Commission's 6th Framework Programme through Contract GOCE-CT-2003-505539. We thank Aart Overeem for providing the confidence bands for the radar data and comments, Geert Lenderink and Erik van Meijgaard for discussions, and Albert Klein Tank for comments on an earlier version.

## Appendix A. Uncertainty assessment and removal of trends

Since the standard errors of the parameters cannot be obtained from the derivatives of the log-likelihood because of the dependence between the precipitation maxima at different grid boxes in the region, a bootstrap procedure described by Hanel et al. (2009) is used to construct confidence intervals for the GEV parameters and the quantiles of the annual maximum distributions. Let $X(s,t)$ be the annual precipitation maximum at grid box $s$ in year $t$. The resampling procedure can be summarized as follows:

1. Calculate the standard Gumbel residuals $\tilde{X}(s,t)$ using:

$$\tilde{X}(s,t) = \frac{1}{\hat{\kappa}(t)} \log\left[1 + \frac{\hat{\kappa}(t)}{\hat{\gamma}(t)}\left(\frac{X(s,t)}{\hat{\xi}(s,t)} - 1\right)\right], \tag{A.1}$$

   where $\hat{\xi}(s,t)$, $\hat{\gamma}(t)$, and $\hat{\kappa}(t)$ are obtained by replacing the parameters $\xi_0(s)$, $\xi_1$, $\gamma_0$, $\gamma_1$, $\kappa_0$, and $\kappa_1$ in Eqs. (4)–(6) by their maximum likelihood estimates $\hat{\xi}_0(s), \hat{\xi}_1, \hat{\gamma}_0, \hat{\gamma}_1, \hat{\kappa}_0$, and $\hat{\kappa}_1$. This transformation removes the trend in the annual maxima. The $\tilde{X}(s,t)$ follow a standard Gumbel distribution, i.e. a Gumbel distribution with $\xi = 0$ and $\alpha = 1$.
2. Draw a sample $t_1, \ldots, t_u, \ldots, t_N$ with replacement from the years $1, \ldots, N$, where $N$ is the number of years (e.g., $N = 149$ in the case of the transient RCM simulations covering the period 1951–2099).
3. Form a bootstrap sample of standard Gumbel residuals by taking the vector $\left(\tilde{X}(1,t_u), \ldots, \tilde{X}(s,t_u), \ldots, \tilde{X}(S,t_u)\right)$ for each resampled year $t_u$ , with $S$ the number of the grid boxes in the region.
4. Transform this bootstrap sample back to the original scale using:

$$X(s,u) = \hat{\xi}(s,u)\left\{1 + \hat{\gamma}(u)\frac{\exp\left[\hat{\kappa}(u)\tilde{X}(s,t_u)\right] - 1}{\hat{\kappa}(u)}\right\}. \tag{A.2}$$

5. Re-estimate the parameters and quantiles.

Steps 2–5 are repeated until the required number of bootstrap samples is obtained.

In the present paper, the transformations (A.1) and (A.2) are also used to remove the trend from the series of the annual precipitation maxima in the transient RCM simulations in order to obtain the area-average quantile plots for the period 1961–1990 shown in Fig. 3. First, the standard Gumbel residuals are calculated as described above. The average time indicator $I(t)$ for the period 1961–1990 is substituted into Eqs. (4)–(6) to obtain estimates of the parameters $\xi$, $\gamma$, and $\kappa$ for that period. These estimates are used in Eq. (A.2) to transform the standard Gumbel residuals to annual precipitation maxima that are representative of the period 1961–1990. These adjusted annual precipitation maxima are then ordered for each grid box, and subsequently the values for each rank are averaged over the 65 grid boxes (pluses in Fig. 3). Likewise, for the fitted GEV model the estimated location parameters are averaged over the 65 grid boxes to obtain one curve for the whole region.

## References

Bell, F.C., 1976. The areal reduction factor in rainfall frequency estimation. Report No. 35, Institute of Hydrology, Wallingford, UK.
Berne, A., Delrieu, G., Creutin, J.-D., Obled, C., 2004. Temporal and spatial resolution of rainfall measurements required for urban hydrology. J. Hydrol. 299, 166–179. doi:10.1016/j.jhydrol.2004.08.002.
Buonomo, E., Jones, R., Huntingford, C., Hannaford, J., 2007. On the robustness of changes in extreme precipitation over Europe from two high resolution climate change simulations. Q. J. R. Meteorol. Soc. 133, 65–81. doi:10.1002/qj.13.
Christensen, O.B., Drews, M., Christensen, J.H., Dethloff, K., Ketelsen, K., Hebestadt, I., Rinke, A., 2007. The HIRHAM regional climate model version 5 (β). DMI Technical Report 06-17, Danish Meteorological Institute, Copenhagen, Denmark.
Collins, M., Booth, B.B.B., Harris, G.R., Murphy, J.M., Sexton, D.M.H., Webb, M.J., 2006. Towards quantifying uncertainty in transient climate change. Clim. Dyn. 27, 127–147. doi:10.1007/s00382-006-0121-0.
Durman, C.F., Gregory, J.M., Hassell, D.C., Jones, R.G., Murphy, J.M., 2001. A comparison of extreme European daily precipitation simulated by a global and regional climate model for present and future climates. Q. J. R. Meteorol. Soc. 127, 1005–1015. doi:10.1002/qj.49712757316.
Fowler, H.J., Ekström, M., 2009. Multi-model ensemble estimates of climate change impacts on UK seasonal precipitation extremes. Int. J. Climatol. 29, 286–416. doi:10.1002/joc.1827.
Fowler, H.J., Ekström, M., Blenkinsop, S., Smith, A.P., 2007. Estimating change in extreme European precipitation using a multimodel ensemble. J. Geophys. Res. 112, D18104. doi:10.1029/2007JD008619.
Frei, C., Schöll, R., Fukutome, S., Schmidli, J., Vidale, P.L., 2006. Future change of precipitation extremes in Europe: Intercomparison of scenarios from regional climate models. J. Geophys. Res. 111, D06105. doi:10.1029/2005JD005965.
Goubanova, K., Li, L., 2007. Extremes in temperature and precipitation around the Mediterranean basin in an ensemble of future climate scenario simulations. Global Planet. Change 57, 27–42. doi:10.1016/j.gloplacha.2004.06.010.
Grum, M., Jørgsen, A.T., Johansen, R.M., Linde, J.J., 2006. The effect of climate change on urban drainage: an evaluation based on regional climate model simulations. Water Sci. Technol. 54(6–7), 9–15. doi:10.2166/wst.2006.592.
Hanel, M., Buishand, T.A., 2010. Analysis of precipitation extremes in an ensemble of transient regional climate model simulations for the Rhine basin. Clim. Dyn., 35. doi:10.1007/s00382-010-0822-2.
Hanel, M., Buishand, T.A., Ferro, C.A.T., 2009. A nonstationary index flood model for precipitation extremes in transient regional climate model simulations. J. Geophys. Res. 114, D15107. doi:10.1029/2009JD011712.
Hershfield, D.M., 1961. Rainfall frequency atlas of the United States for durations from 30 minutes to 24 hours and return periods from 1 to 100 years. Weather Bureau Technical Paper No. 40, US Department of Commerce, Washington, DC.
Hewitt, C.D., Griggs, D.J., 2004. Ensembles-based predictions of climate changes and their impacts. Eos 85 (52), 566. doi:10.1029/2004EO520005.
Hosking, J.R.M., Wallis, J.R., 1997. Regional Frequency Analysis. Cambridge University Press, New York.
Jacob, D. et al., 2001. A comprehensive model intercomparison study investigating the water budget during the BALTEX-PIDCAP period. Meteorol. Atmos. Phys. 77 (1-4), 19–43. doi:10.1007/s007030170015.
Jones, R.G., Noguer, M., Hassell, D.C., Hudson, D., Wilson, S.S., Jenkins, G.J., Mitchell, J.F.B., 2004. Generating High Resolution Climate Change Scenarios Using PRECIS. Met Office Hadley Centre, Exeter, UK.
Jungclaus, J.H., Keenlyside, N., Botzet, M., Haak, H., Luo, J.-J., Latif, M., Marotzke, J., Mikolajewicz, U., Roeckner, E., 2006. Ocean circulation and tropical variability in the coupled model ECHAM5/MPI-OM. J. Clim. 19, 3952–3972. doi:10.1175/JCLI3827.1.
Kjellström, E., Bärring, L., Gollvik, S., Hansson, U., Jones, C., Samuelsson, P., Rummukainen, M., Ullerstig, A., Willén, U., Wyser, K., 2005. A 140-year simulation of European climate with the new version of the Rossby Centre regional atmospheric climate model (RCA3). SMHI Reports Meteorology and Climatology 108, Swedish Meteorological and Hydrological Institute, Norrköping, Sweden.
Koutsoyiannis, D., 2004. Statistics of extremes and estimation of extreme rainfall: II. empirical investigation of long rainfall records. Hydrol. Sci. J. 49, 581–610.
Lenderink, G., van Meijgaard, E., 2008. Increase in hourly precipitation extremes beyond expectations from temperature changes. Nat. Geosci. 1, 511–514. doi:10.1038/ngeo262.
NERC, 1975. Flood Studies Report. Natural Environment Research Council, London, UK.

Olsson, J., Berggeren, K., Olofsson, M., Viklander, M., 2009. Applying climate model precipitation scenarios for urban hydrological assessment: a case study in Kalmar City, Sweden. Atmos. Res. 92, 364–375. doi:10.1016/j.atmosres.2009.01.015.

Onof, C., Arnbjerg-Nielsen, K., 2009. Quantification of anticipated future changes in high resolution design rainfall for urban areas. Atmos. Res. 92, 350–363. doi:10.1016/j.atmosres.2009.01.014.

Overeem, A., Buishand, A., Holleman, I., 2008. Rainfall depth–duration–frequency curves and their uncertainties. J. Hydrol. 348, 124–134. doi:10.1016/j.jhydrol.2007.09.044.

Overeem, A., Buishand, T.A., Holleman, I., 2009a. Extreme rainfall analysis and estimation of depth-duration-frequency curves using weather radar. Water Resour. Res. 45, W10424. doi:10.1029/2009WR007869.

Overeem, A., Holleman, I., Buishand, A., 2009b. Derivation of a 10-year radar-based climatology of rainfall. J. Appl. Meteorol. Climatol. 48, 1448–1463. doi:10.1175/2009JAMC1954.1.

Overeem, A., Buishand, T.A., Holleman, I., Uijlenhoet, R., in press. Extreme-value modeling of areal rainfall from weather radar. Water Resour. Res., 46.

Salas-Mélia, D., Chauvin, F., Déqué, M., Douville, H., Gueremy, J.F., Marquet, P., Planton, S., Royer, J.F., Tyteca, S., 2005. Description and validation of the CNRM-CM3 global coupled model. CNRM Working Note 103, National Center for Meteorol. Research, Toulouse, France.

Schilling, W., 1991. Rainfall data for urban hydrology: what do we need? Atmos. Res. 27, 5–21. doi:10.1016/0169-8095(91)90003-F.

Uppala, S.M. et al., 2005. The ERA-40 re-analysis. Q. J. R. Meteorol. Soc. 131, 2961–3012. doi:10.1256/qj.04.176.

van Meijgaard, E., van Ulft, L.H., van de Berg, W.J., Bosveld, F.C., van den Hurk, B.J.J.M., Lenderink, G., Siebesma, A.P., 2008. The KNMI regional atmospheric climate model RACMO, Version 2.1. KNMI Technical Report 302, Royal Netherlands Meteorological Institute, De Bilt, The Netherlands.

van Montfort, M.A.J., 1990. Sliding maxima. J. Hydrol. 118, 77–85.